International Journal of Pharmaceutics 400 (2010) 183–193

Contents lists available at ScienceDirect

International Journal of Pharmaceutics

journal homepage: www.elsevier.com/locate/ijpharm

Pharmaceutical Nanotechnology

Tight junction modulation by chitosan nanoparticles: Comparison with chitosan solution

Driton Vllasaliu[a,1], Ruth Exposito-Harris[b,1], Angeles Heras[b], Luca Casettari[a,c], Martin Garnett[a], Lisbeth Illum[d], Snow Stolnik[a,*]

[a] The School of Pharmacy, Boots Science Building, University of Nottingham, University Park, Nottingham NG7 2RD, United Kingdom
[b] Institute for Biofunctional Studies, Physical Chemistry Department, Faculty of Pharmacy, Complutense University of Madrid, Madrid, Spain
[c] Pharmaceutical Chemistry Institute, University of Urbino 'Carlo Bo', Urbino 61029, Italy
[d] Critical Pharmaceuticals, BioCity Nottingham, Pennyfoot Street, Nottingham NG1 1GF, United Kingdom

ARTICLE INFO

Article history:
Received 11 January 2010
Received in revised form 12 August 2010
Accepted 13 August 2010
Available online 19 August 2010

Keywords:
Chitosan
Calu-3
Permeation enhancer
Nanoparticles
Tight junction modulation
Nasal drug delivery

ABSTRACT

Present work investigates the potential of chitosan nanoparticles, formulated by the ionic gelation with tripolyphosphate (TPP), to open the cellular tight junctions and in doing so, improve the permeability of model macromolecules. A comparison is made with chitosan solution at equivalent concentrations. Initial work assessed cytotoxicity (through MTS and LDH assays) of chitosan nanoparticles and solutions on Calu-3 cells. Subsequently, a concentration of chitosan nanoparticles and solution exhibiting minimal toxicity was used to investigate the effect on TEER and macromolecular permeability across filter-cultured Calu-3 monolayer. Chitosan nanoparticles and solution were also tested for their effect on the distribution of the tight junction protein, zonnula occludens-1 (ZO-1). Chitosan nanoparticles produced a sharp and reversible decrease in TEER and increased the permeability of two FITC-dextrans (FDs), FD4 (MW 4 kDa) and FD10 (MW 10 kDa), with effects of a similar magnitude to chitosan solution. Chitosan nanoparticles produced changes in ZO-1 distribution similar to chitosan solution, indicating a tight junction effect. While there was no improvement in permeability with chitosan nanoparticles compared to solution, nanoparticles provide the potential for drug incorporation, and hence the possibility for providing controlled drug release and protection from enzymatic degradation.

1. Introduction

The development of therapeutics based on biotechnology products is a rapidly expanding area within the pharmaceutical industry. A recent report by the Pharmaceutical Research and Manufacturers of America (PhRMA) states that in 2008 there were 633 biotechnology medicines in development for more than 100 diseases. However, this growth is not matched by development of novel delivery systems for this class of therapeutics. Currently, most biomolecules are predominantly administered parenterally. This is due to their large size, hydrophilicity and their inability to withstand the environment in the gastrointestinal tract, resulting in an inadequate absorption, and hence bioavailability, following oral administration. However, disadvantages associated with the parenteral route such as patients' non-compliance, necessitate research into alternative ways of administering these drugs.

The delivery of biomolecular therapeutics, such proteins, antibodies and nucleic acids via the nasal cavity is attractive due to the relatively large surface area available for absorption (~150 cm^2), the highly vascularised submucosa, and the avoidance of both gastric and first pass metabolism (Illum, 2000). However, there are several biological barriers to the transport of biomolecules across the nasal mucosa, including a functional mucociliary clearance mechanism, which results in removal of foreign material from the nasal mucosa within 15–20 min, the presence of proteases that may degrade the administered protein drug and the existence of tight junctions between adjacent epithelial cells, severely limiting the permeability of macromolecules larger than 1000 Da (Illum, 2000; Stolnik and Shakesheff, 2009).

It has been shown that chitosan is able to considerably enhance the nasal absorption of macromolecules, including peptides and proteins, which are otherwise poorly absorbed. Chitosan is a cationic polymer (polysaccharide) produced by partial deacetylation of chitin and has been reported to be biocompatible, biodegradable and exhibiting a low toxicity (Hirano et al., 1990; Dornish et al., 1996; Grenha et al., 2007). Its absorption-promoting effect is thought to result from a combination of mucoadhesion and the ability to open the intercellular tight junctions (Artursson et al.,

* Corresponding author. Tel.: +44 1158 466074; fax: +44 1159 515102.
E-mail address: snjezana.stolnik@nottingham.ac.uk (S. Stolnik).
[1] These authors contributed equally to the paper.

0378-5173/$ – see front matter © 2010 Published by Elsevier B.V.
doi:10.1016/j.ijpharm.2010.08.020

1994; Illum, 1998; Dyer et al., 2002). The mucoadhesive properties of chitosan have been attributed mainly to an interaction between its positively charged amino groups with negatively charged sialic acid groups on the mucus membrane (Fiebrig et al., 1994). Application of therapeutic agents in combination with chitosan has been reported to prolong the contact time between the agent and the absorptive surface for up to 84 min in man for a chitosan powder formulation (Soane et al., 1999). The capacity of chitosan to transiently open the tight junctions has been associated with an interaction of chitosan with the Protein Kinase C pathway (Smith et al., 2005).

Different chitosan formulations, such as solutions, freeze dried or spray dried powders and nanoparticles have been investigated for the potential improvement of nasal absorption of various macromolecular drugs (Dyer et al., 2002; Illum, 2007). While chitosan solution and powder formulations improve mucosal absorption through mucoadhesion and tight junction-modulation, chitosan nanoparticle formulations have been developed in an attempt, to deliver macromolecules across mucosal surfaces by exploiting endocytic/transcytotic pathways (Fernandez-Urrusuno et al., 1999; Behrens et al., 2002; Vila et al., 2002). Potential advantages associated with the use of chitosan nanoparticles encompass entrapment of the drug within the particle matrix, consequently ensuring protection against enzymatic degradation that may occur at the mucosal surface and the possibility of controlled drug release. However, despite these potential advantages, so far only one published study has shown superior mucosal drug absorption using chitosan nanoparticles compared to chitosan solution (Fernandez-Urrusuno et al., 1999).

Dyer et al. (2002) showed that in the rat and sheep models, the pharmacological responses to an insulin-chitosan solution or insulin-chitosan powder formulation applied nasally were significantly higher compared to those resulting from an equivalent chitosan nanoparticle formulation. Similarly, Ma and Lim (2003) showed that chitosan nanoparticles did not mediate translocation of insulin across intestinal Caco-2 cell layers. Recently Sadeghi et al. (2008) found that chitosan (and its derivatives) in a nanoparticulate form were less efficient in opening the tight junctions than their soluble form equivalents. The authors suggested that drug movement across the cell layers would be more likely to occur through the transcellular pathway rather than as a result of tight junction opening.

The present work set out to investigate the potential of chitosan nanoparticles, formulated by the ionic gelation method, to improve the permeability of macromolecular compounds across biological membranes through tight junction modulation, in comparison to the soluble equivalent. Initial work assessed the effects of increasing concentrations of chitosan nanoparticles and solutions on cell toxicity. The concentrations exhibiting minimal and reversible toxicity were then used to investigate tight junction modulation and macromolecular permeability. The *in vitro* mucosal model in this work was based on a filter-cultured Calu-3 cell line. Although the Calu-3 cell line is of a human lung (bronchial carcinoma) origin its use in this work as a model of the nasal epithelium was considered as appropriate. Calu-3 cells, when cultured under the conditions employed in this work, form a polarized cell layer and establish a mixed phenotype, including ciliated and secreting cells, with physical and electrical properties comparable to nasal mucosa (Witschi and Mrsny, 1999; Florea et al., 2002). Indeed, Calu-3 cell cultures have previously been used to study nasal drug absorption (Yang et al., 2004; Li et al., 2006; Seki et al., 2007; Teijeiro-Osorio et al., 2009a,b). The artificial tracheo-bronchial tissue, EpiAirway®, has also been used to investigate nasal drug absorption *in vitro* (Agu et al., 2004; Chemuturi et al., 2005). Furthermore, Calu-3 cells produce mucus when cultured using appropriate conditions (Florea et al., 2002) which were employed in this work.

2. Materials and methods

2.1. Materials

Chitosan in the form of a hydrochloride salt of average molecular weight 113 kDa and deacetylation degree 86% (commercially known as Protasan® UP Cl 113), referred to as 'chitosan' in this paper, was purchased from NovoMatrix, Norway. Calu-3 cells and Eagle's Minimal Essential Medium (EMEM) were obtained from the American Type Culture Collection (ATCC)–LGC Promochem. Caco-2 cells were obtained from European Collection of Cell Cultures (ECACC). Calu-3 and Caco-2 cells were used between passages 19–48 and 44–58, respectively. Dulbeco's Modified Eagles Medium (DMEM), Hanks Balanced Salt Solution (HBSS, with sodium bicarbonate and without phenol red), Pentasodium tripolyphosphate (TPP), non-essential amino acids (100%), L-glutamine (200 mM), foetal bovine serum (FBS), antibiotic/antimycotic solution (10–12,000 U/ml penicillin, 10–12 mg/ml streptomycin, 25–30 μg/ml amphotericin B), trypsin–EDTA solution (2.5 mg/ml trypsin, 0.2 mg/ml EDTA), Cibacron Brilliant Red and fluorescein isothiocyanate-labelled dextrans (FITC-dextrans, FDs) of molecular weights 4000 (FD4) and 10,000 (FD10) and LDH assay kit (commercial name TOX7) were all supplied by Sigma–Aldrich (Poole, UK). Fluorescin isothiocyanate (FITC, Type I) was purchased from Molecular Probes (Paisley, UK). MTS reagent, 3-(4,5-dimethylthiazol-2-yl)-5(3-carboxymethonyphenol)-2-(4-sulfophenyl)-2H-tetrazolium (commercially known as CellTiter 96® AQ_{ueous} One Solution Cell Proliferation Assay) was purchased from Promega (USA). Mouse anti-human Zonnula Occludens-1 (ZO-1; tight junction protein) antibody was purchased from Zymed (part of Invitrogen). FITC-labelled goat anti-mouse IgG, 4-(2-hydroxyethyl)piperazine-1-ethanesulfonic acid solution (HEPES) and 2-(*N*-morpholino)ethanesulfonic acid (MES) were obtained from Sigma. Tissue culture flasks (75 cm^3 with ventilated caps), black 96-well plates and Transwell inserts (12 mm diameter, 0.4 μm pore size, were purchased from Costar (High Wycombe, UK). ProLong® Gold antifade reagent with 4′,6-diamidino-2-phenylindole (DAPI) was obtained from Invitrogen. Phosphate buffered saline (PBS) tablets were purchased from Oxoid (Basingstoke, UK). All other chemicals (reagent grade) were purchased form Sigma–Aldrich.

2.2. Methods

2.2.1. Chitosan nanoparticles preparation

Chitosan nanoparticles were prepared by the ionic gelation of tripolyphosphate pentasodium (TPP) and chitosan hydrochloride, as described by Fernandez-Urrusuno et al. (1999) and Dyer et al. (2002). Preliminary experiments were performed with the objective of identifying the optimal concentrations (ratios) of chitosan and TPP for nanoparticle formation (appearance of an opalescent suspension). Chitosan hydrochloride solutions (2, 1.5, 1, 0.75 and 0.5 mg/ml) and TPP solution (0.84 mg/ml) were prepared in ultrapure water. TPP solution was added dropwise to chitosan solution while stirring. The resultant mixtures were broadly characterized as either a clear solution, an opalescent mixture or phase-separated aggregates. The formation of nanoparticles was confirmed by particle size analysis (Dynamic Light Scattering, Viscotek, UK). Excess chitosan was removed by centrifugation (at 13,000 rpm, for 30 min); the supernatant was tested for the presence of chitosan using a colorimetric method, as described by Muzzarelli (1998) and centrifugation was repeated until chitosan could no longer be detected. The concentration of chitosan present in nanoparticles was determined by quantifying chitosan in the supernatant following the centrifugation steps and subtracting this from the starting amount used for nanoparticle formulation.

2.2.2. Particle characterization

The mean diameter and size distribution of chitosan nanoparticles, suspended in HBSS (MES buffered at pH 6.0) were measured by DLS. The result represents the mean of 10 measurements, performed at 25 °C. Zeta potential of the nanoparticles (suspended in HBSS, pH 6.0) was measured using a Zetasizer, 2000 (Malvern Instruments, UK). The reported value is the mean of four measurements ±SD.

2.2.3. Synthesis of FITC-chitosan

FITC-chitosan was synthesized according to a method described by Colonna et al. (2008). Chitosan (100 mg) was dissolved in deionized water (10 ml), followed by the addition of DMSO (20 ml) to this solution. FITC (5 mg), previously dissolved in DMSO, was slowly added to the resulting chitosan solution under continuous stirring. The reaction was carried out overnight at room temperature in the dark. The resulting solution was poured in an excess of acetone and then centrifuged for 10 min at 3000 rpm. The pellet was washed several times with fresh acetone. Following each washing step, acetone (washing solution) was tested for FITC fluorescence using a Hitachi F-4500 fluorescence spectrophotometer (Hitachi Scientific Instruments, Finchamstead, UK). Washing was continued until a FITC fluorescence signal was no longer observed in the washing solution. The pellet was then dissolved in water and dialysed against deionised water using a 1000 Da molecular weight cut off (MWCO) membrane for three days while protected from light. The FITC-labelled chitosan was then freeze dried.

2.2.4. Formulation of FITC-chitosan nanoparticles

FITC-chitosan nanoparticles were produced using the ionic gelation technique in a similar way to unlabelled chitosan nanoparticles. The optimal polymer:TPP ratio was found to be between 6:1 and 4:1.

2.2.5. Cell culture

Calu-3 cells were cultured to confluence in 75 cm^3 flasks at 5% CO_2, 37 °C. Once confluent, they were detached from the flasks and seeded on filter inserts (Transwells®) at a density of 100,000 cells/cm^2. Cells were maintained at 5% CO_2, 37 °C in EMEM supplemented with FBS (10%) antibiotic/antimycotic and L-glutamine, which was changed regularly (every other day). Air–liquid interface (ALI) was created on day two of culture of cells of filters (i.e. following this time point, cells were cultured with no medium present on the apical surface). Cell growth and tight junction formation was assessed by TEER measurements. Cell layers were typically used for TEER and permeability experiments between days 8 and 10 in culture.

Caco-2 cells were cultured in flasks using DMEM as the growth medium. Upon confluence, cells were seeded on filters at a density of 100,000 cells/cm^2. Caco-2 cells were cultured on filters using submerged (or liquid covered culture, LCC) conditions, with replacement of the culture medium every other day. Cells were cultured for 21–23 days prior to their use as cell layers in TEER experiment.

2.2.6. MTS toxicity assay

The MTS colorimetric assay was performed to evaluate the effect of chitosan nanoparticles on cell viability in comparison with chitosan solution. Furthermore, this test was undertaken in order to identify the highest concentration of nanoparticles (and solution) that exhibited insignificant toxicity towards Calu-3 cells. Calu-3 cells were seeded on 96-well plates at a density of 10,000 cells per well and cultured in the EMEM medium for 24 h. Prior to the test, cell medium was removed and replaced by sample solutions comprising of chitosan nanoparticles or chitosan solution at concentrations of 0.025%, 0.0125%, 0.006125%, 0.003% and 0.0015% (w/v) in HBSS (MES-buffered, pH 6.0). Triton X-100 (0.1%, v/v in MES-buffered HBSS, pH 6.0) and HBSS (MES-buffered, pH 6.0) were used as a positive and negative control, respectively. Cells were incubated (at 37 °C, 5% CO_2) with samples and controls for a period of 2 h. Samples (and controls) were then removed and cells washed with PBS. The MTS assay was subsequently conducted according to the manufacturer's instructions, with at least four repeats for each sample.

In order to assess whether cells recover following the application of chitosan, a further MTS assay was performed 15 h after cells were exposed to the chitosan samples (incubated for 2 h, as in the previous test). In the period between removal of the chitosan samples (nanoparticles and solution) and the MTS assay, cells were incubated with EMEM (at 37 °C, 5% CO_2).

Finally, to test whether the medium in which chitosan nanoparticles were suspended changed the toxicity profile of chitosan, the MTS assay was performed with nanoparticles resuspended in cell culture medium (EMEM, without FCS) and this was compared with HBSS. Cells were incubated with these samples for 2 h, following which the MTS assay was performed in the same way as above.

The relative cell viability (%) was calculated using the following equation:

$$\text{Viability} = \frac{S - T}{H - T} \times 100$$

$$\text{Viability} = \frac{S - T}{H - T} \times 100$$

S = viability obtained with the tested samples; T = viability observed with Triton X-100; H = viability with HBSS.

2.2.7. LDH release assay

Lactate dehydrogenase (LDH) release assay was conducted to assess whether chitosan nanoparticles or chitosan solution exhibited any membrane disruptive-effects. Cells were seeded on 96-well plates at a seeding density of 10,000 cells per well and incubated in the cell medium (EMEM) for 24 h (at 37 °C, 5% CO_2). The tested samples (chitosan nanoparticles and solution) and controls were then applied to cells in the same manner as for the MTS assay (detailed above). The LDH leakage test was then conducted according to the manufacturer's protocol. The relative LDH release was calculated as the percentage relative to the controls, using the following equation,

$$\text{Relative LDH toxicity} = \frac{S - H}{T - H} \times 100$$

$$\text{Relative LDH toxicity} = \frac{S - H}{T - H} \times 100$$

where S = LDH release with tested samples; H = LDH release in HBSS; T = LDH release with Triton X-100. The test was repeated four times for each sample.

2.2.8. TEER experiments

Calu-3 and Caco-2 cell layers exhibiting TEER ≥500 Ωcm^2 and ≥400 Ωcm^2, respectively (referred to as 'electrically resistant' in this paper) were used in these experiments. Prior to sample application, cell medium was removed and replaced with HBSS (buffered at pH 6.0 with MES and pH 7.4 with HEPES on the apical and basolateral sides of the cell layers, respectively). Cells were equilibrated in HBSS (incubated at 37 °C, 5% CO_2) for ~45 min, following which TEER was measured; this was treated as the baseline TEER. Chitosan nanoparticles and chitosan solution (visually transparent in HBSS at pH 6.0) were then applied to the apical side of the cell layers at different concentrations and cells were incubated with the samples for 2 h. TEER was measured at times 0.5, 1, 1.5 and 2 h (in

the presence of the tested chitosan samples, in HBSS) following the sample application. The samples were removed after 2 h and cells washed extensively with PBS. Cell medium was then added to both sides of the cell layers. A further measurement of TEER was taken (with cells bathed in medium) at time 4 h following the exposure of the cells with chitosan. Cells were then incubated with the culture medium (EMEM and DMEM for Calu-3 and Caco-2 cells, respectively), overnight (air–liquid interface culture conditions were used for Calu-3 cells). TEER measurements were conducted the next day, 22 h after the application of chitosan to the cell layers in order to determine whether the changes in TEER (if any) were reversible. TEER was measured using an EVOM Voltohmmeter (World Precision Instruments, UK), equipped with a pair of chopstick electrodes. Cell layers incubated with HBSS (buffered at pH 6.0 and 7.4 on the apical and basolateral side, respectively) for 2 h and with EMEM (overnight) were used as the reference and the changes in TEER are reported as percentage relative to this reference. Background TEER due to the filter (~100 to 110 Ωcm^2) was deducted from the measurements in all cases. All experiments were performed in triplicates.

2.2.9. Association of FITC-chitosan nanoparticles with Calu-3 cell layers

FITC-chitosan nanoparticles were suspended in HBSS (MES-buffered, pH 6.0) to a concentration of 0.003% (w/v) chitosan and then applied to the apical side of electrically resistant (TEER $\geq$500 Ωcm^2) Calu-3 cell layers previously equilibrated in HBSS. Cells were incubated with FITC-chitosan nanoparticles at 37 °C for 2 h. Nanoparticle suspensions were then removed and cells washed extensively with PBS. Cell layer-containing filters were then excised and mounted (using DAPI-containing ProLong® Gold antifade/mounting medium) on glass slides for confocal imaging. Cells were imaged using a Leica TCS SP2 system mounted on a Leica DMIRE2 inverted microscope.

2.2.10. Effect of chitosan nanoparticles and solution on ZO-1 distribution

Chitosan in nanoparticulate or solution form of 0.003% (w/v) concentration (in HBSS, pH 6.0), was applied to the apical side of electrically resistant Calu-3 cell layers, following an equilibration step with HBSS. Cells were incubated with chitosan nanoparticles or solution for a period of 2 h followed by cell washing with PBS. Cells were then fixed with 4% paraformaldehyde in PBS for 5–10 min, washed with PBS and permeabilized with Triton X-100 (0.1%, v/v in PBS) for ~10 min. Triton X-100 solution was thereafter removed and cells washed with PBS. 1% BSA in PBS was applied to the cell layers and an incubation period of 45 min-1 h was allowed. Thereafter, this solution was aspirated and replaced with mouse anti-human ZO-1 (primary) antibody, diluted in 1% BSA/PBS to a final concentration of 10 mg/ml. Cell samples were incubated with the primary antibody for 1 h. The primary antibody solution was then removed and cells extensively washed with PBS. FITC-labelled goat anti-mouse (secondary) antibody, diluted to 2 mg/ml in 1% BSA/PBS was then applied to the cells for 1 h. The secondary antibody solution was aspirated and cells washed extensively. The filter membrane was excised and mounted on a glass slide for confocal imaging, as described previously.

2.2.11. Permeability experiments

Fluorescein isothiocyanate (FITC)-labelled dextrans of molecular weight 4400 (FD4) and 10,000 (FD10) were used as models for hydrophilic drug macromolecules. Calu-3 cells were cultured using air–liquid interface conditions on filters as described above and only cell layers with TEER $\geq$500 Ωcm^2 were used for the purpose of this experiment. Prior to sample application, cell medium (EMEM) was removed and the cell layers washed with PBS. Cells were then equilibrated in HBSS (buffered to pH 6.0 and 7.4 on the apical and basolateral sides, respectively) for a period of ~45 min. Chitosan nanoparticles or chitosan solution, at a final concentration of 0.003% (w/v) in HBSS (pH 6.0), and FD4 or FD10 at a final concentration of 500 μl/ml (in HBSS, pH 6.0), were then applied (in combination) to the apical side of the cells. Basolateral solution was sampled (100 μl volumes) at the following time points: 30, 60, 90, 120, 150 and 180 min after chitosan/FD application, and the sampled volume replaced with fresh HBSS. FITC-dextrans in the sampled basolateral solution were quantified by fluorescence, using an MFX microtiter plate fluorometer (Dynex Technologies, USA). After the final sampling, chitosan nanoparticles or solution and the FITC-dextrans were removed from the cells. The cell layers were then washed with PBS and the normal cell medium applied. Cell layers were then incubated overnight, following which the TEER was measured in order to ensure that the cell layer integrity was not compromised during the permeability experiments and that cells recover. The permeability of FITC-dextrans is expressed as the apparent permeability coefficient (P_{app}), calculated using the following equation:

$$P_{app} = \left(\frac{\Delta Q}{\Delta t}\right) \times \left(\frac{1}{A \times C_0}\right)$$

$$P_{app} = \left(\frac{\Delta Q}{\Delta t}\right) \times \left(\frac{1}{A \times C_0}\right)$$

P_{app}, apparent permeability (cm/s); $\Delta Q/\Delta t$, permeability rate (amount of FD traversing the cell layers over time); A, diffusion area of the layer (cm^2); C_0, apically added FITC-dextran concentration. The experiment was conducted in triplicates.

2.2.12. Statistical analysis

Statistical comparisons were performed by Student's t-test. Values of $p < 0.05$ were considered statistically significant.

3. Results

3.1. Chitosan nanoparticles production and characterisation

Following the initial screening experiments, the optimised preparation conditions (initial concentrations of chitosan and the polyphosphate salt) were identified as a final chitosan hydrochloride concentration of 1.5 mg/ml and a final TPP concentration of 1.8 mg/ml. Under these conditions, the formed nanoparticles had a mean hydrodynamic radius of 339 ± 66 nm (Fig. 1) as measured in HBSS (pH 6.0). The particles size profile further reveals a presence of another particle populations (mean hydrodynamic radius approximately 34 nm and in the range of 10–0 μm). These particulates comprised a small fraction of the overall nanoparticle suspension and are thought to result from uncomplexed chitosan and aggregated nanoparticles.

Nanopartricles had a surface potential of +11.3 ± 2.7 mV in HBSS (pH 6.0). The final nanoparticles suspension, after the removal of excess free chitosan, following the procedure described in the methods section, contained 0.56 ± 0.06 mg/ml of chitosan (in the form of nanoparticles), as determined by the colorimetric assay.

3.2. MTS (toxicity) assay

The effect of chitosan nanoparticles and chitosan solution on the relative cell viability of Calu-3 cells is shown in Fig. 2. Nanoparticle suspensions containing 0.0015% and 0.003% (w/v) chitosan show no significant suppressive effect on Calu-3 viability, while nanoparticle suspensions containing chitosan concentrations >0.006% (w/v) all exhibit significant reductions (>50%) in relative cell viability in a

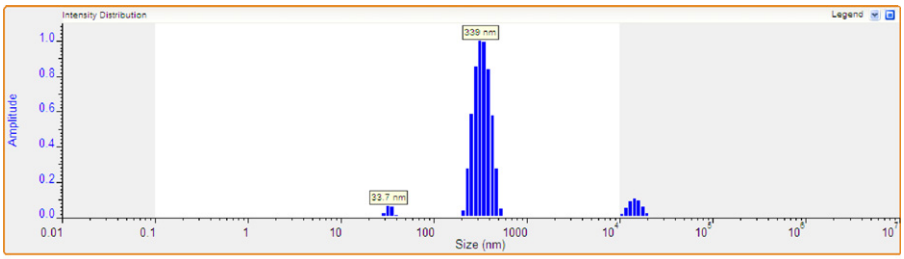

	% Area	Rh (nm)	Position	Std Dev	% RSD
1	2	33.68	32.36	2.38	7.1
2	98	339.4	316.23	66.73	19.7

Fig. 1. Dynamic Light Scattering (DLS) measurement of the size distribution of chitosan nanoparticles suspended in HBSS (pH 6.0). The result represents a mean of 10 measurements, performed at 25 °C.

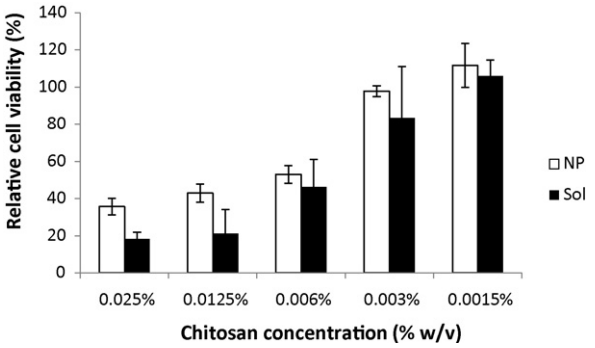

Fig. 2. Effect of chitosan nanoparticles and chitosan solution on the viability of Calu-3 cells, measured by the MTS assay following a 2-h incubation of the cells with chitosan samples. Results presented as % viability relative to controls (HBSS and Triton X-100) and expressed as the mean ± SD ($n = 5$).

concentration-dependent manner. It should be noted that chitosan solutions at two highest concentrations (0.0125% and 0.025%, w/v) exhibit significantly higher suppressive effect than corresponding nanoparticle concentrations, while for the lower three concentrations (0.006%, 0.003% and 0.0015%, w/v), although the reduction in cell viability appears higher for chitosan solution, this difference is not statistically significant. According to this study, one can assign 0.003% (w/v) as the highest chitosan concentration, for both solution and nanoparticles, exhibiting no statistically significant suppression on cell viability, as determined by the MTS assay.

The recovery of cells following the application of chitosan nanoparticles and solution was also tested (Fig. 3) by conducting the MTS assay 13 h following the exposure of the cells to chitosan. Although the data variability is higher than in Fig. 2, it can nevertheless be noticed that in this cell recovery experiment, chitosan nanoparticle suspensions were typically associated with higher cell viability, relative to chitosan solutions of the corresponding concentration. Namely, for chitosan nanoparticles statistically higher relative cell viability was observed for 0.003% and 0.0015% (w/v) tested concentrations, compared to chitosan solution.

In order to assess a potential effect that the incubation medium in which chitosan nanoparticles were presented to the cells may have had on the toxicity profile, the effect on cell viability was compared for chitosan nanoparticle suspensions applied in either HBSS (pH 6.0), a medium typically used for in vitro drug transport studies, or serum-free cell medium (EMEM at pH 6.0), which is the recommended medium for Calu-3 cells. Fig. 4 clearly depicts that the nature of the incubation medium has a remarkable effect on the level of cell toxicity exhibited. In the EMEM medium, only an application of chitosan nanoparticles at concentrations of 0.1% and 0.05% (w/v) caused a statistically significant reduction in relative cell viability, whereby the effect appears to be concentration dependent. Suspended in HBSS, all concentrations of chitosan nanoparticles caused statistically significant and high reductions in relative cell viability (Fig. 2).

3.3. LDH assay

Fig. 5 shows the effect of chitosan nanoparticles and chitosan solution on relative LDH toxicity. The release of LDH from cells is generally considered as an indication of plasma membrane disruption. In essence, a concentration-dependent toxicity was found for both chitosan nanoparticles and chitosan solution (apart from the highest concentrations of chitosan solution). Application of nanoparticle suspension equivalent to chitosan concentration of 0.003% (w/v), identified using the MTS assay as the highest con-

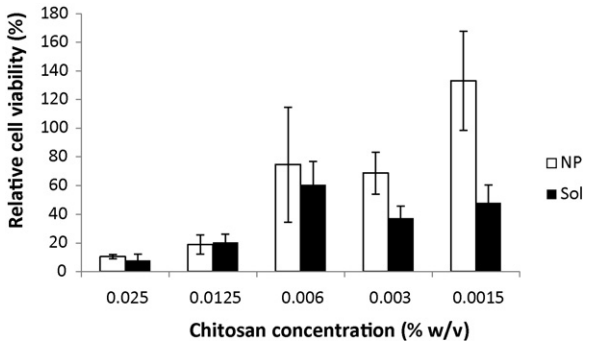

Fig. 3. Long term effect of chitosan nanoparticles and chitosan solution on the viability of Calu-3 cells, measured by the MTS assay 13 h following the incubation of cells with chitosan samples. Results presented as % viability relative to controls (HBSS and Triton X-100) and expressed as the mean ± SD ($n = 5$).

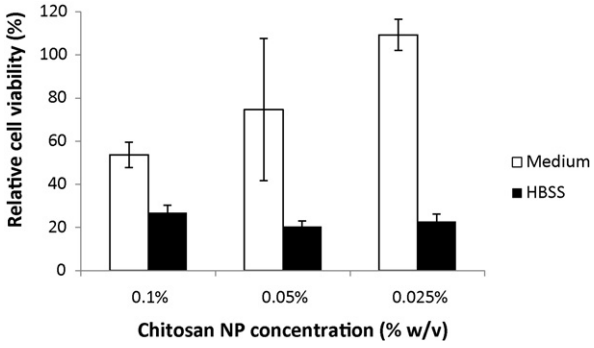

Fig. 4. Effect of nanoparticle (NP) suspension medium on cell viability measured by the MTS assay following a 2-h incubation of cells with chitosan NPs suspended in HBSS or serum-free EMEM ('medium'). Results presented as % viability relative to controls (HBSS and Triton X-100) and expressed as the mean ± SD ($n = 5$).

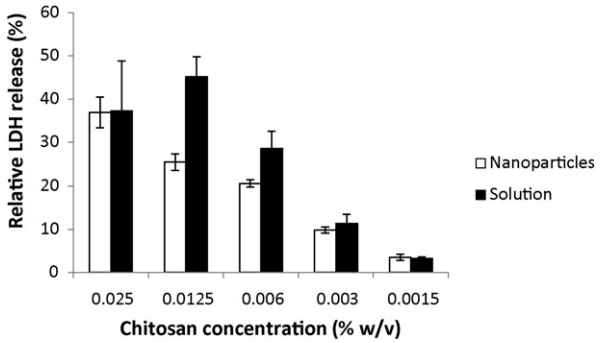

Fig. 5. Effect of chitosan nanoparticles and solution on LDH leakage following a 2-h incubation of cells with samples. Results expressed as LDH release relative to that obtained with Triton X-100 (0.1%, v/v in HBSS) and presented as the mean ± SD (n = 4).

centration that did not affect cell viability, caused a 10% increase in LDH release, compared to controls, whereas chitosan solution of the same concentration showed an increase of 11%. Both these values are significantly different to the HBSS control, indicating higher membrane disruption, however there is no statistically significant difference between chitosan nanoparticles and solution (p = 0.33). Applying higher concentrations, the membrane toxicity gradually increased for both systems, reaching approximately 54% and 62% of LDH release of Triton X-100 (positive control) with nanoparticles (at 0.025%, w/v) and solution (at 0.0125%, w/v), respectively. At the higher concentrations of nanoparticles and solution, 0.006% and 0.0125% (w/v), there is a statistically significant difference (p = 0.043 and p = 0.004 for 0.006%, w/v and 0.0125%, w/v, respectively), whereby at the same chitosan concentration solutions showed higher membrane toxicity.

3.4. TEER experiments

The effect of chitosan nanoparticles and chitosan solutions of two different concentrations (0.003% and 0.006%, w/v) on the TEER of the Calu-3 layers is presented in Fig. 6 (Fig. 6a and b for chitosan nanoparticles and chitosan solution, respectively). Both profiles exhibit a typical pattern of a steep decrease in TEER to <10% of the baseline value for all the samples applied. TEER remained low (in the region <10% of the baseline figure) for the duration of cell incubation with the samples (2 h). The largest recorded decrease in TEER is, however, significantly (statistic significance) larger for chitosan solution than for the nanoparticles.

Reversibility of TEER following the removal of chitosan formulations from the cell layers was found to be concentration dependent, whereby the higher concentration of chitosan nanoparticles and solution (0.006%, w/v) was associated with an irreversible lowering of the TEER (Fig. 6a and b). Measured 20 h after subjecting the cell layers to chitosan incubation, the TEER values were in the order of 10% and 5% of the baseline figure, respectively. TEER values for 0.003% (w/v) nanoparticle suspension showed a high level of recovery (to 92% of the baseline value) in the same time period (Fig. 6a). Regarding chitosan solution, the concentration of 0.003% (w/v) again showed recovery, with TEER reaching 84% of the baseline value (Fig. 6b). An interesting point to note is that the lower concentration (0.003%, w/v chitosan) produced an initial TEER reduction similar in magnitude to that of the higher concentration (0.006%, w/v) with which no recovery was observed.

In order to determine whether the TEER-reducing effect of chitosan nanoparticles was reproducible in a different cell line that also forms electrically tight cell layers, this effect was tested on intestinal Caco-2 cells. Fig. 7 shows that the application of chitosan nanoparticles to Caco-2 layers was again associated with a decrease

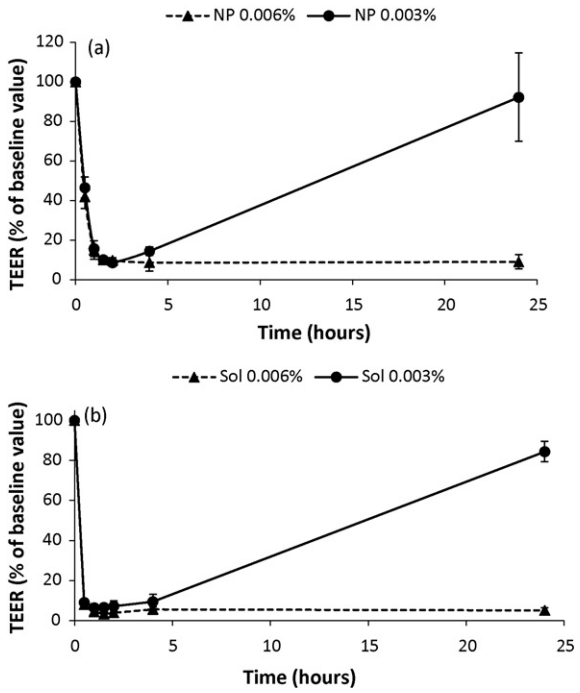

Fig. 6. Effect of chitosan nanoparticles (NPs) (a) and solution (Sol) (b) on Calu-3 cell layer TEER. Chitosan NPs and chitosan solutions were used at concentrations 0.003% (w/v) and 0.006% (w/v). Time 0 h represents baseline TEER (i.e. TEER in HBSS, prior to application of chitosan samples). Arrows indicate chitosan sample removal and replacement with cell medium. Results presented as the mean ± SD (n = 3).

in TEER and that the extent of this reduction was similar to Calu-3 cells. TEER recovery was again dependent upon the nanoparticle concentration. However, importantly, in Caco-2 cells a complete TEER recovery (tested 22 h after a 2 h incubation of cells with chitosan nanoparticles) was observed with a 0.0125%, w/v chitosan concentration of nanoparticles. This is a four times higher concentration of material than the chitosan nanoparticle concentration exhibiting a reversible TEER reduction in Calu-3 cells. Furthermore, a partial TEER recovery was also evident with higher nanoparticle concentrations (to 64%, 53% and 29% of baseline value with nanoparticle concentrations containing chitosan concentrations of 0.025%, 0.05% and 0.1%, w/v, respectively).

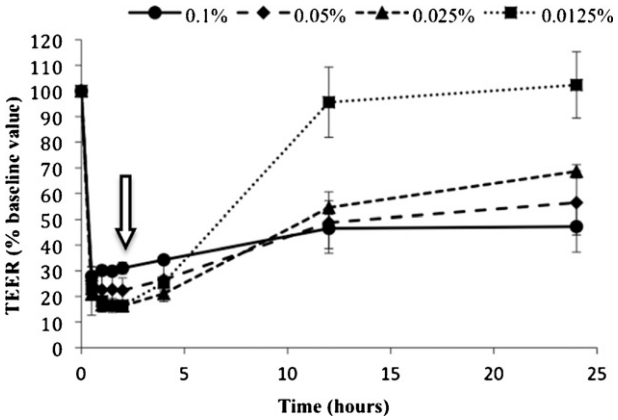

Fig. 7. Effect of chitosan NPs on Caco-2 cell layer TEER. Chitosan NPs were applied to cells at concentrations 0.1%, 0.05%, 0.025% and 0.0125% (w/v). Time 0 h represents baseline TEER (i.e. TEER in HBSS, prior to application of chitosan NPs). Arrow indicates sample removal and replacement with cell medium. Results presented as the mean ± SD (n = 3).

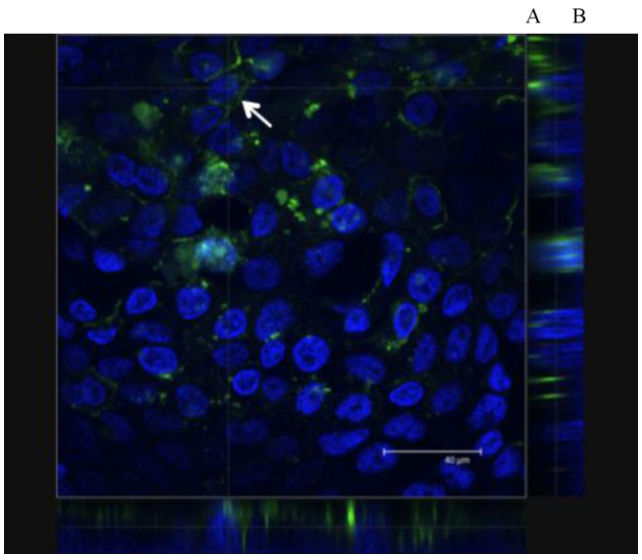

Fig. 8. Association of FITC-chitosan nanoparticles with Calu-3 cells. Green: FITC-labelled nanoparticles and blue: DAPI-labelled cell nuclei. Apical side of the cells is marked with A, whereas basolateral side is marked with B.

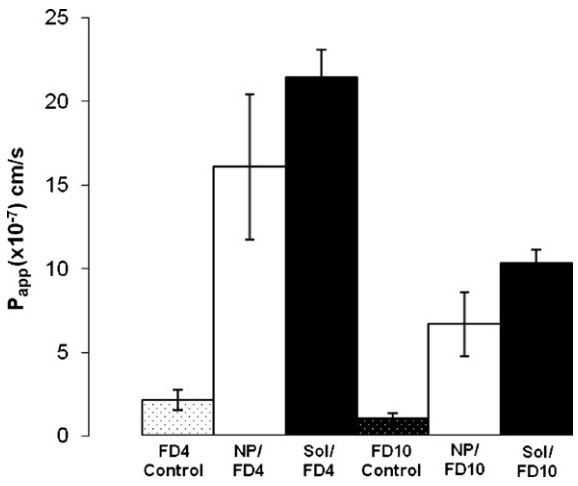

Fig. 10. Effect of chitosan nanoparticles (NPs) and solution on the permeability of FD4 and FD10 across Calu-3 layers. Control represents FD4 and FD10 permeability without the presence of chitosan NPs or chitosan solution. Permeability expressed as apparent permeability coefficient (P_{app}), Results expressed as the mean ± SD ($n = 4$).

3.5. Association of FITC-chitosan nanoparticles with Calu-3 cell layers

The association of FITC-chitosan nanoparticles with Calu-3 cells, following incubation and extensive cells washing, is shown in Fig. 8. Green fluorescence, arising from FITC-labelled chitosan nanoparticles is distributed throughout the imaged area of the cell layer. In some regions the fluorescence is concentrated, forming larger aggregates, while in other regions, punctate fluorescence indicating nano-sized species (nanoparticles), could be observed. In some regions (arrow) the fluorescence appears to follow the contour of cells on the apical surface. With respect to nanoparticle fluorescence distribution across the vertical axis of the cell layer, nanoparticles were mainly observed on the apical side of the cells (marked A), with some nanoparticle fluorescence also observed deeper, within the level of the cell nuclei and closer to the basolateral surface of the cells (marked B).

3.6. Effect of chitosan nanoparticles and solution on ZO-1 distribution

Structural changes at the level of the cellular tight junctions resulting from the application of chitosan as nanoparticles and solution are shown in Fig. 9. A continuous ring of fluorescence, arising from ZO-1 staining, at cell-cell contacts is clearly visible in the control cell layer (Fig. 9a). Fluorescence at the point of contact between the cells can also be seen in cell layers incubated with chitosan nanoparticles (Fig. 9b) and solution (Fig. 9c). However, in comparison to the control cell layers, a considerable loss in continued fluorescence is clearly apparent, with observation of discontinuous pericellular rings of fluorescence for both, chitosan nanoparticles and chitosan solution.

3.7. FD permeability across Calu-3 layers

The permeability study was conducted to compare suspension of chitosan nanoparticles and a corresponding solution containing 0.003% (w/v) of chitosan. The selection was based on (i) the low toxicity of this chitosan concentration, as determined by the MTS assays, and (ii) the finding that this was the highest chitosan concentration that showed reversibility in TEER *versus* time profile, for both formulations. Two FITC-dextrans (FD4 and FD10) were selected as macromolecular permeants (model drugs) and the effect of chitosan nanoparticles and solution of the equivalent concentration on their permeability was compared (Fig. 10). The data clearly demonstrate that chitosan nanoparticles significantly enhance the permeability of both FD4 and FD10, relative to the control. The extent of this effect is apparently dependent

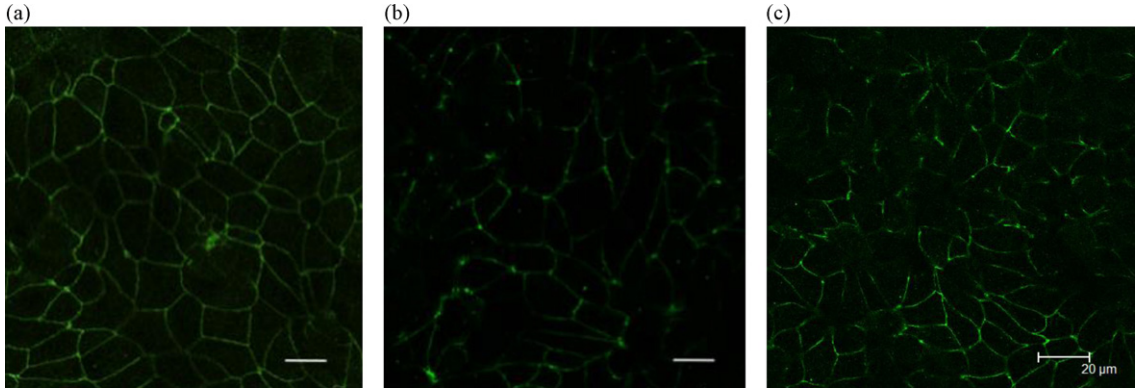

Fig. 9. Effect of chitosan on distribution of ZO-1 tight junction protein in Calu-3 cell layers. (a) ZO-1 staining in control cell layers not subjected to chitosan incubation (white line represents a scale bar of 10 µm), (b) ZO-1 staining in cells incubated with NPs of 0.003% (w/v) chitosan (white line represents a scale bar of 10 µm), and (c) ZO-1 distribution in cell layers incubated with chitosan solution, 0.003% (w/v). ZO-1 immunostaining was performed in the same way (see Section 2.2) for all conditions.

on the molecular weight of the FITC-dextran; the permeability of FD4 is enhanced 7.6-fold while there is a 6.5-fold increase in the permeability of FD10. Chitosan solution appears more efficient in improving the permeability of both FD4 and FD10, with a 10.1-fold improvement in permeability across the cells observed for both FITC-dextrans, relative to their respective controls. However the difference between chitosan nanoparticles and solution for the effect on FD4 transport was found to be statistically insignificant ($p = 0.074$), though the data obtained are highly variable. In contrast, the improvement in FD10 permeability achieved with chitosan solution is significantly ($p = 0.018$) higher than for the nanoparticles. The data therefore clearly show that in the presence of chitosan nanoparticles, the FITC-dextrans (coexisting in the same solution and not incorporated within the nanoparticles) exhibit paracellular translocation across the Calu-3 layers and that this translocation is dependent upon the molecular size.

4. Discussion

The mucoadhesive and tight junction opening functionalities of chitosan have especially been exploited in formulation of nasal macromolecular therapeutics, including peptides and proteins (Illum, 2003). In addition to the well-documented tight junction opening and mucoadhesive properties of chitosan solutions (Smith et al., 2005; Soane et al., 1999), it has been suggested that chitosan nanoparticles, and nanoparticles of other materials, may improve mucosal absorption by traversing the epithelial barriers. The concept of using nano-sized carriers to transport drugs across the epithelial layers, however remains controversial (Illum, 2007). The *in vivo* transport of 150–200 nm polylethylene glycol coated polylactide/glycolide nanoparticles in the absence of any permeability enhancer was suggested by Vila et al. (2002), although no evidence was shown of *in vitro* nanoparticle translocation, or indeed of a systemic effect of insulin *in vivo*, from insulin–chitosan complex nanoparticles following nasal administration (Mao et al., 2005). It has also been suggested that a paracellular transport of nanoparticles larger than 20 nm is not feasible due to a maximal widening of the intercellular spaces of about 15 nm (Jung et al., 2000). The efficacy of mucosal absorption of macromolecules using chitosan nanoparticles as a carrier system has in general been shown to be inferior compared to that obtained with chitosan solution or chitosan powder formulations (Dyer et al., 2002; Illum, 2007). While some studies have reported opening of tight junctions by chitosan nanoparticles, other investigations have shown no such effects, as discussed later.

The present work provides a comparison between the effect of chitosan nanoparticles and solution on tight junction opening, whereby the paracellular translocation of model therapeutic macromolecules across the mucosal surfaces is investigated. In this study the hydrophilic FITC-dextrans (FD4 and FD10), serving as models for therapeutic biomacromolecules, were not incorporated within the interior of the chitosan nanoparticles, but applied to cells in conjunction with the chitosan solution and the nanoparticle suspension. This work therefore mimics a possible situation where the therapeutic macromolecule is released from, and resides at the mucosal surface alongside the nanoparticles. FITC-dextrans (FD4 and FD10) are transported across a cell monolayer via the tight junctions only but due to their large size the extent of this transport is small. However their paracellular transport would be improved if the chitosan formulations exhibited a tight junction-opening effect. The present experimental design eliminated the need to consider a contribution of possible transcellular transport of chitosan nanoparticles on the overall translocation of macromolecules across the epithelial cell layer. Even if transcellular transport of chitosan nanoparticles did occur, this would not contribute to the apical-to-basolateral translocation of the FITC-dextrans.

Chitosan nanoparticles were in this work prepared by the ionic gelation method, under relatively mild preparation conditions, which would enable incorporation of different therapeutic molecules (including labile protein macromolecules) within the interior of the nanoparticles. Previous studies have incorporated several biomolecules, in addition to peptides and protein, including tetanus toxoid (Sayin et al., 2008) and siRNA (Katas and Alpar, 2006) into similarly fabricated nanoparticles. The concentrations of chitosan and TPP established as optimal for the production of nanoparticles in this experiment are comparable to those reported previously (Calvo et al., 1997), with the final chitosan and TPP concentrations in the order of 1–3 mg/ml and 0.2–1.0 mg/ml, respectively. The optimal chitosan:TPP ratio on a weight-to-weight basis in this study was found to be 4.0, which is again comparable to the above studies. The zeta potential of the chitosan nanoparticles was, as expected, positive, under experimental conditions used in the measurements, which is believed to be important for maintaining the mucoadhesive and tight junction-opening properties of chitosan (Schipper et al., 1997). It should be noted that the preparation of chitosan nanoparticles was based on the interaction between positively charged chitosan groups and the negatively charged TPP, where a balanced ratio of the two compounds is needed to ensure both sufficient cross-linking and also nanoparticle charge stabilization and surface presence of excess charge. It was ensured by centrifuging and repeated washing of the nanoparticles that no free chitosan was present in the nanoparticle formulations, which could have biased the results. In previous studies by other research groups it has often not been clear whether free chitosan was present in the formulations and hence these studies are not directly comparable with this work.

Systematic studies on cell toxicity (using two different cell toxicity assays, MTS and LDH assays, and in addition an assessment of cell layer integrity through measurement of TEER) were conducted in this work to compare the effects of chitosan nanoparticles with corresponding concentrations of chitosan solutions. From these studies the concentration of chitosan (in nanoparticulate and solution form) with minimal toxic effects and a reversible decrease in cell layer TEER was chosen. Performing such a selection was considered necessary in order to ensure that the observed effects on TEER and permeability were due to tight junction opening and a resulting increased access to the paracellular route, and not because of cell toxicity and compromised cell layer integrity.

It is interesting to note that the effect of chitosan nanoparticles on Calu-3 cell viability, as observed by the MTS assay, was slightly lower compared to chitosan solution. While in some cases this difference did not reach a statistical significance, in other scenarios this discrepancy was clearly apparent.

The data on the membrane-disruptive effects of chitosan nanoparticles, as determined by the LDH assay, indicate that even at chitosan concentration of as low as 0.003% (w/v), chitosan nanoparticles exhibit some degree of membrane disruption. A similar effect is observed with chitosan solution of an equivalent concentration. Although there are a large number of reported studies on the permeability-promoting effect of chitosan, very few of these studies incorporated the LDH membrane toxicity test. Silva et al. (2006) found that application of chitosan solutions (MW 150 kDa and degree of deacetylation near 85%) to Caco-2 cells was associated with dose-dependent and significant membrane toxicity. The concentrations of chitosan used in these studies were 0.1%, 0.25% and 0.5% (w/v). In another study, a 30 min exposure of Caco-2 cell layers with chitosan hydrochloride, used at concentrations 0.005%, 0.01% and 0.5% (w/v), resulted in a slight increase in extracellular LDH activity. However, when cells were allowed to recover for 8 h or 24 h following the incubation with 0.005% or 0.01% (w/v) con-

centrations of chitosan, the LDH activity at these time points was similar to control, suggesting cell membrane recovery. Schipper et al. (1996) found a dose-dependent effect on intracellular dehydrogenase release from Caco-2 cells when exposed to chitosans having a low degree of acetylation (<35%).

It should be noted that the concentrations of chitosan, either in solution or nanoparticle form, used in this study (0.003% and 0.006%, w/v) were significantly lower than those typically reported in the literature. Reports on the toxicity of chitosan on Calu-3 cells are sparse, despite chitosan being studied extensively as a mucoadhesive and permeability-enhancing agent. It has been reported that application of chitosan solution at a concentration of 1.5% (w/v) reduced the viability of Calu-3 cells to around 68% compared to control (Florea et al., 2006). Chitosan nanoparticles prepared by a similar ionic gelation method, as used in the present study, were shown to induce a reduction in the viability of A549 cells (human alveolar epithelial carcinoma) to approximately 70% at a concentration of around 1 mg/ml (0.1%, w/v) (Huang et al., 2004). The same authors also reported that chitosan, delivered as microparticles, induced pro-inflammatory responses in rat lungs (Huang et al., 2005). However, other studies have reported a low toxicity of chitosan solution and nanoparticles in respiratory cell lines (Grenha et al., 2007; Smith et al., 2005). In a recent publication, the authors noted that chitosan/cyclodextrin ('hybrid') nanoparticles exhibited a significantly lower cytotoxicity than those based on chitosan only (Teijeiro-Osorio et al., 2009a,b), whereby the IC_{50} values (nanoparticle dose causing a 50% reduction in cell viability) were 3-fold higher for chitosan/cyclodextrin-containing nanoparticles compared to the chitosan-only nanoparticles. However, it should be emphasized that direct comparisons between these studies, and also with the present work, is problematic due to the variabilities in the experimental parameters, including the use of different cytotoxicity assays, cell lines, different conditions employed, different chitosan forms, molecular weights and suppliers, and finally, differences in chitosan formulations.

Regarding the cell line variabilities, our study clearly demonstrates a significant difference in sensitivity towards chitosan in Caco-2 and Calu-3 cell lines, which are typically used in the research area. Reversibility in TEER (indicating cell layer recovery) was seen in Caco-2 cells following nanoparticle application containing significantly higher concentrations of chitosan compared to that used in Calu-3 cells. This indicates a cell specific toxicity and emphasizes the importance of using a relevant cell culture model.

The TEER data in this study demonstrates that chitosan in nanoparticulate form, as *per* production method described, maintains its intrinsic capacity to open the cellular tight junctions. Application of chitosan nanoparticles or chitosan solution to Calu-3 cell layers are shown both to be associated with a dramatic decrease in TEER, whereby the effect of nanoparticle formulation is comparable, although somewhat reduced, to chitosan solution of a corresponding concentration. Our results are in discrepancy with a study by Ma and Lim (2003), where soluble chitosan was more effective at disrupting the intercellular tight junction than chitosan nanoparticles. This was explained by the possibility of a less effective interaction of chitosan nanoparticles with the cellular proteins because of their TPP-crosslinked chains (Ma and Lim, 2003). Furthermore, in a recent publication investigating the effect of chitosan-TPP nanoparticles incorporated into mannitol microspheres on tight junction modulation of Calu-3 layers, the authors did not observe any effects (on TEER and permeability) for the maximum nanoparticle concentration tested (1.3 mg/ml of nanoparticles in the formulation, corresponding to chitosan amount of 150 μg) (Grenha et al., 2007). Discrepancy in the capacity to induce tight junction opening between chitosan solution and nanoparticles has also been explained by a restriction in the movement of the chitosan chains in the nanoparticulate form, hindering the contact of these chains with the plasma membranes and tight junctions (Prego et al., 2005).

Another recent study on the effect of chitosan solution and nanoparticle formulations on TEER of Caco-2 layers (Sadeghi et al., 2008) showed that, in comparison to the free-soluble polymers, nanoparticles based on chitosan and its quaternized derivatives (prepared by the ionic gelation method as used in this study), had a much lower effect on decreasing the TEER. The authors explained the finding by the reduced available amount of positive charge (charge density) at the surface of the nanoparticles, compared to the soluble form of chitosan.

In the present study an equivalent amount of chitosan in the nanoparticulate form (devoid of free chitosan) to that in the solution form was applied and therefore the argument that there would be a reduced exposure of positive charge in the nanoparticles in comparison to the solution would stand. The tight junction modulating effects of chitosan were shown to be mediated by its cationic charges in a study by Schipper et al. (1997), where the authors demonstrate an inhibition of permeation enhancement of chitosan by addition of the highly negatively charged heparin. The same group also showed (Schipper et al., 1996) that chitosans with a lower degree of deacetylation, and therefore with less free positively charged amino groups, had a lower absorption promoting effect.

Furthermore, the potential inferior capacity of chitosan in a nanoparticulate form to open the tight junctions, compared to the soluble form, has been attributed to the difference in calcium biding capacity between nanoparticles and solution. Poly(isobutyl cyanoacrylate) core-shell nanoparticles coated with chitosan were shown to possess a higher capacity to bind calcium than the solution, which the authors explained by an improvement in the accessibility of binding sites of chitosan on the nanoparticle surface (Bravo-Osuna et al., 2007). This results in a higher calcium-depleting capacity of nanoparticles compared to solution. However, despite the widely acknowledged role of calcium in maintaining the tight junction integrity and therefore the barrier property of the epithelium (Rabito et al., 1978; Ma et al., 2000), previous work by our group has shown that a reduction of apical calcium levels in Caco-2 and Calu-3 cell layers leads to a limited effect on tight junction opening with a reversible TEER decrease and a very limited increase in FD4 permeability (Vllasaliu et al., 2008).

The present study uses mucus producing, air–liquid interface cultured Calu-3 cell layers. The presence of mucus would be expected to promote association of chitosan nanoparticles, as well as chitosan from solution, with the mucus. Behrens et al. (2002) demonstrated a strong association of chitosan nanoparticles (prepared by the same method as in the present study) with mucus-secreting MTX-E12 cells (58%), an effect that was less apparent with non-mucus producing Caco-2 cells (7.8%). Their study further showed that the largest fraction of nanoparticles was bound to mucus and that removal of the mucus layer prior to incubation of cells with nanoparticles led to a 14% decrease of nanoparticle association with the cells.

The strong mucoadhesive properties of chitosan coated-poly(isobutylcyanoacrylate) nanoparticles have also been suggested by Bravo-Osuna et al. (2008). However, in this study, the authors argue that the mucoadhesive properties of chitosan-coated nanoparticles lead to their immobilization in the mucus layer, and in doing so, hamper their diffusion within the layer, reaching the vicinity of the tight junction proteins, which the authors consider to be a prerequisite for a tight junction-modulating effect. This theory was provided as an explanation for their finding that chitosan-coated nanoparticles were ineffective in opening of the tight junctions and improving the paracellular permeability.

In our study, confocal imaging of the cell layers incubated with nanoparticles formulated with FITC-labelled chitosan showed

nanoparticle distribution throughout the viewed area of the cell layer. The widespread observation of chitosan nanoparticles on the apical side of the cell layer, even after extensive washing of the cells, indicates a strong association of the nanoparticles with the cell layer possibly arising due to mucoadhesion and/or bioadhesion, which is in agreement with the above study. However, in our study, chitosan nanoparticles appear to reach the apical cell membrane level, with some evidence of nanoparticle uptake, as judged from observations of vertical (Z-sections) distribution of fluorescence in Fig. 8. This suggests a close proximity of the nanoparticles to the apical cell membrane and cellular tight junctions, enabling an interaction of chitosan with the tight junction proteins and the resulting tight junction opening effect clearly demonstrated in this work.

Determination of structural changes in cellular tight junctions following the incubation of the cells with chitosan formulations (nanoparticles and solution) revealed that chitosan nanoparticles produced a change in the distribution of ZO-1 protein that was similar to that observed with chitosan solution, if not greater. Importantly, this experiment showed that the TEER-reducing and permeability-enhancing effects of chitosan nanoparticles do indeed result from an effect on tight junctions and, to our knowledge, no previous studies in the literature had reported such structural changes in tight junctions with chitosan nanoparticles.

Owing to the bioadhesive nature of chitosan nanoparticles, which is demonstrated in this work, any tight junction-opening effect that the nanoparticles may have is therefore likely to be relatively sustainable. Provided that the therapeutic molecule is present in the vicinity (i.e. released from the nanoparticle), the mucoadhesive and tight junction opening effect of chitosan nanoparticles would be expected to result in an improvement of its permeability across the mucosal surface.

Our experiments evaluating the apical-to-basolateral translocation of two hydrophilic macromolecules across the Calu-3 cell layers show that chitosan nanoparticles, devoid of free chitosan, significantly enhanced the permeability. In the case of the smaller permeant macromolecule, FD4, the increase in permeability seen with chitosan nanoparticles was similar to that observed with chitosan solution of corresponding concentration. For the transport of FD10, a significantly higher apparent permeability is seen with chitosan solution compared to nanoparticles. It is not clear whether this may be due to the somewhat lower effect of chitosan nanoparticles on TEER reduction, compared to chitosan solution, although the images in Fig. 9 do not indicate substantial difference in the effect of solution and nanoparticles effect on ZO-1 protein.

The present work therefore clearly demonstrates that chitosan nanoparticles, devoid of free chitosan, reversibly open the tight junctions and enhance macromolecular permeability across a bronchial epithelial cell line (Calu-3), without inducing irreversible toxicity to the cells at the optimized concentration used. Furthermore, the data shows that chitosan nanoparticles have a permeability-increasing effect similar to chitosan solution for a 4 kDa macromolecular permeant and somewhat inferior effect for a 10 kDa macromolecule. Although the work shows there is no improvement in permeability-enhancement of chitosan nanoparticles compared to chitosan solution, it may be still advantageous to deliver biomacromolecular drugs via the mucosal surfaces by incorporating them within the nanoparticles with the aim to provide protection from enzymatic degradation, prolong the presence time with the mucosa and achieve a controlled drug release.

5. Conclusions

The work presented here shows the ability of chitosan nanoparticles to open the cellular tight junctions and consequently improve the permeability of model macromolecules. Comparing with chitosan solution at equivalent concentrations, the data demonstrate that chitosan nanoparticles produced a sharp and reversible decrease in TEER and increased the permeability of two model permeants, FITC-dextrans of 4 and 10 kDa, to a similar magnitude to chitosan solution. Chitosan nanoparticles produced changes in ZO-1 (tight junction protein) distribution similar to chitosan solution, indicating a tight junction effect. While chitosan nanoparticles did not demonstrate an improvement in permeability, compared to the solution, nanoparticles afford the potential for drug incorporation and therefore controlled drug release and protection from enzymatic degradation at mucosal surface.

References

Agu, R.U., Valiveti, S., et al., 2004. Intranasal delivery of recombinant human parathyroid hormone [hPTH(1-34)], teriparatide in rats. Endocr. Res. 30 (3), 455–467.

Artursson, P., Lindmark, T., et al., 1994. Effect of chitosan on the permeability of monolayers of intestinal epithelial cells (Caco-2). Pharm. Res. 11 (9), 1358–1361.

Behrens, I., Pena, A.I., et al., 2002. Comparative uptake studies of bioadhesive and non-bioadhesive nanoparticles in human intestinal cell lines and rats: the effect of mucus on particle adsorption and transport. Pharm. Res. 19 (8), 1185–1193.

Bravo-Osuna, I., Millotti, G., et al., 2007. In vitro evaluation of calcium binding capacity of chitosan and thiolated chitosan poly(isobutyl cyanoacrylate) core–shell nanoparticles. Int. J. Pharm. 338 (1–2), 284–290.

Bravo-Osuna, I., Vauthier, C., et al., 2008. Specific permeability modulation of intestinal paracellular pathway by chitosan-poly(isobutylcyanoacrylate) core-shell nanoparticles. Eur. J. Pharm. Biopharm. 69, 436–444.

Calvo, P., Remunan-Lopez, C., et al., 1997. Novel hydrophylic chitosan-polyethylene oxide nanoparticles as protein carriers. J. Appl. Polym. Sci. 63, 125–132.

Chemuturi, N.V., Hayden, P., et al., 2005. Comparison of human tracheal/bronchial epithelial cell culture and bovine nasal respiratory explants for nasal drug transport studies. J. Pharm. Sci. 94 (9), 1976–1985.

Colonna, C., Conti, B., et al., 2008. Ex vivo evaluation of prolidase loaded chitosan nanoparticles for the enzyme replacement therapy. Eur. J. Pharm. Biopharm. 70, 58–65.

Dornish, M., Aarnold, M., et al., 1996. Alginate and chitosan: Biodegradable biopolymers in drug delivery systems. Eur. J. Pharm. Sci. 4, S153.

Dyer, A.M., Hinchcliffe, M., et al., 2002. Nasal delivery of insulin using novel chitosan based formulations: a comparative study in two animal models between simple chitosan formulations and chitosan nanoparticles. Pharm. Res. 19 (7), 998–1008.

Fernandez-Urrusuno, R., Calvo, P., et al., 1999. Enhancement of nasal absorption of insulin using chitosan nanoparticles. Pharm. Res. 16 (10), 1576–1581.

Florea, B.I., Meaney, C., et al., 2002. Transfection efficiency and toxicity of polyethylenimine in differentiated Calu-3 and non differentiated COS-1 cell cultures. AAPS Pharm. Sci. 4 (3), E12.

Florea, B.I., Thanou, M., et al., 2006. Enhancement of bronchial octreotide absorption by chitosan and N-trimethyl chitosan shows linear in vitro/in vivo correlation. J. Control Release 110 (2), 353–361.

Fiebrig, I., Harding, S.E., et al., 1994. Sedimentation analysis of potential interaction between mucins and a putative bioadhesive polymer. Progr. Colloid Polym. Sci. 94, 66–73.

Grenha, A., Grainger, C.I., et al., 2007. Chitosan nanoparticles are compatible with respiratory epithelial cells in vitro. Eur. J. Pharm. Sci. 31 (2), 73–84.

Hirano, S., Seino, H., et al., 1990. Chitosan: a biocompatible material for oral and intravenous administration. In: Gebelein, C.G., Dunn, R.L. (Eds.), Progress in Biomedical Polymers. Plenum Press, New York, pp. 283–289.

Huang, M., Khor, E., et al., 2004. Uptake and cytotoxicity of chitosan molecules and nanoparticles: effects of molecular weight and degree of deacetylation. Pharm. Res. 21 (2), 344–353.

Huang, Y.C., Vieira, A., et al., 2005. Pulmonary inflammation caused by chitosan microparticles. J. Biomed. Mater. Res. A 75 (2), 283–287.

Illum, L., 1998. Chitosan and its use as a pharmaceutical excipient. Pharm. Res. 15 (9), 1326–1331.

Illum, L., 2000. Transport of drugs from the nasal cavity to the central nervous system. Eur. J. Pharm. Sci. 11 (1), 1–18.

Illum, L., 2003. Nasal drug delivery–possibilities, problems and solutions. J. Control. Release. 87, 187–198.

Illum, L., 2007. Nanoparticulate systems for nasal delivery of drugs: a real improvement over simple systems? J. Pharm. Sci. 96 (3), 473–483.

Jung, T., Kamm, W., et al., 2000. Biodegradable nanoparticles for oral delivery of peptides: is there a role for polymers to affect mucosal uptake? Eur. J. Pharm. Biopharm. 50, 147–160.

Katas, H., Alpar, H.O., 2006. Development and characterization of chitosan nanoparticles for siRNA delivery. J. Control Release 115 (2), 216–225.

Li, L., Mathias, N.R., et al., 2006. Carbopol-mediated paracellular transport enhancement in Calu-3 cell layers. J. Pharm. Sci. 95 (2), 326–335.

Ma, T.Y., Tran, D., et al., 2000. Mechanism of extracellular calcium regulation of intestinal epithelial tight junction permeability: role of cytoskeletal involvement. Microsc. Res. Tech. 51, 156–168.

Ma, Z., Lim, L.Y., 2003. Uptake of chitosan and associated insulin in Caco-2 cell monolayers: a comparison between chitosan molecules and chitosan nanoparticles. Pharm. Res. 20 (11), 1812–1819.
Mao, S., Germershaus, O., et al., 2005. Uptake and transport of PEG-graft-trimethyl-chitosan copolymer-insulin nanocomplexes by epithelial cells. Pharm. Res. 22 (12), 2058–2068.
Muzzarelli, R.A., 1998. Colorimetric determination of chitosan. Anal. Biochem. 260 (2), 255–257.
Prego, C., Garcia, M., et al., 2005. Transmucosal macromolecular drug delivery. J. Control. Release. 101, 151–162.
Rabito, C.A., Rotunno, C.A., et al., 1978. Amiloride and calcium effect on the outer barrier of the frog skin. J. Membr. Biol. 42, 169–187.
Sadeghi, A.M., Dorkoosh, F.A., et al., 2008. Permeation enhancer effect of chitosan and chitosan derivatives: comparison of formulations as soluble polymers and nanoparticulate systems on insulin absorption in Caco-2 cells. Eur. J. Pharm. Biopharm. 70 (1), 270–278.
Sayin, B., Somavarapu, S., et al., 2008. Mono-N-carboxymethyl chitosan (MCC) and N-trimethyl chitosan (TMC) nanoparticles for non-invasive vaccine delivery. Int. J. Pharm. 363 (1–2), 139–148.
Schipper, N.G., Olsson, S., et al., 1997. Chitosans as absorption enhancers for poorly absorbable drugs 2: mechanism of absorption enhancement. Pharm. Res. 14 (7), 923–929.
Schipper, N.G., Varum, K.M., et al., 1996. Chitosans as absorption enhancers for poorly absorbable drugs.1:Influence of molecular weight and degree of acetylation on drug transport across human intestinal epithelial (Caco-2) cells. Pharm. Res. 13 (11), 1686–1692.
Seki, T., Kanbayashi, H., et al., 2007. Effects of asperminated gelatin on the nasal absorption of insulin. Int. J. Pharm. 338 (1–2), 213–218.
Silva, C.M., Veiga, F., et al., 2006. Effect of chitosan-coated alginate microspheres on the permeability of Caco-2 cell monolayers. Drug. Dev. Ind. Pharm. 32, 1079–1088.
Smith, J.M., Dornish, M., et al., 2005. Involvement of protein kinase C in chitosan glutamate-mediated tight junction disruption. Biomaterials 26 (16), 3269–3276.
Soane, R.J., Frier, M., et al., 1999. Evaluation of the clearance characteristics of bioadhesive systems in humans. Int. J. Pharm. 178, 55–65.
Stolnik, S., Shakesheff, K., 2009. Formulations for delivery of therapeutic proteins. Biotechnol. Lett. 31 (1), 1–11.
Teijeiro-Osorio, D., Remunan-Lopez, C., et al., 2009a. Chitosan/cyclodextrin nanoparticles can efficiently transfect the airway epithelium in vitro. Eur. J. Pharm. Biopharm. 71 (2), 257–263.
Teijeiro-Osorio, D., Remunan-Lopez, C., et al., 2009b. New generation of hybrid poly/oligosaccharide nanoparticles as carriers for the nasal delivery of macromolecules. Biomacromolecules 10 (2), 243–249.
Vila, A., Sanchez, A., et al., 2002. Design of biodegradable particles for protein delivery. J. Control Release 78 (1–3), 15–24.
Vllasaliu, D., Garnett, M., et al., 2008. Enhancing Paracellular Permeability by Calcium Depletion. Poster presentation, 2nd International Symposium Cellular Delivery of Therapeutic Macromolecules (CDTM), Cardiff University, UK.
Witschi, C., Mrsny, R.J., 1999. In vitro evaluation of microparticles and polymer gels for use as nasal platforms for protein delivery. Pharm. Res. 16 (3), 382–390.
Yang, T., Hussain, A., et al., 2004. Cyclodextrins in nasal delivery of low-molecular-weight heparins: in vivo and in vitro studies. Pharm. Res. 21 (7), 1127–1136.